Supplemental material to this article can be found at:
http://dmd.aspetjournals.org/content/suppl/2019/07/26/dmd.119.087395.DC1
1521-009X/47/10/1164–1173$35.00
https://doi.org/10.1124/dmd.119.087395
Drug Metabolism and Disposition
Drug Metab Dispos 47:1164–1173, October 2019

Special Section on Pharmacokinetic and Drug Metabolism Properties of Novel Therapeutic Modalities

Metabolism and Disposition of Volanesorsen, a 2′-*O*-(2 methoxyethyl) Antisense Oligonucleotide, Across Species

Noah Post, Rosie Yu, Sarah Greenlee, Hans Gaus, Eunju Hurh, John Matson, and Yanfeng Wang

PK and Clinical Pharmacology (N.P., R.Y., S.G., J.M., Y.W.) and Medicinal Chemistry (H.G.), Ionis Pharmaceuticals, Inc., Carlsbad, California; and PK and Clinical Pharmacology, Akcea Therapeutics, Boston, Massachusetts (E.H.)

Received April 2, 2019; accepted July 24, 2019

ABSTRACT

Volanesorsen (previously known as ISIS 304801) is a 20-nucleotide partially 2′-*O*-(2-methoxyethyl) (2′-MOE)–modified antisense oligonucleotide (ASO) gapmer, which was recently approved in the European Union as a novel, first-in-class treatment in the reduction of triglyceride levels in patients with familial chylomicronemia syndrome. We characterized the absorption, distribution, metabolism, and excretion characteristics of volanesorsen in mice, rats, monkeys, and humans, in either radiolabeled or nonradiolabeled studies. This also included the characterization of all of the observed ASO metabolite species excreted in urine. Volanesorsen is highly bound to plasma proteins that are similar in mice, monkeys, and humans. In all species, plasma concentrations declined in a multiphasic fashion, characterized by a relatively fast initial distribution phase and then a much slower terminal elimination phase following subcutaneous bolus administration. The plasma metabolite profiles of volanesorsen are similar across species, with volanesorsen as the major component. Various shortened oligonucleotide metabolites (5–19 nucleotides long) were identified in tissues in the multiple-dose mouse and monkey studies, but fewer in the [^{3}H]-volanesorsen rat study, likely due to a lower accumulation of metabolites following a single dose in rats. In urine, all metabolites identified in tissues were observed, consistent with both endo- and exonuclease-mediated metabolism and urinary excretion being the major elimination pathway for volanesorsen and its metabolites.

SIGNIFICANCE STATEMENT

We characterized the absorption, distribution, metabolism, and excretion (ADME) of volanesorsen, a partially 2′-MOE–modified antisense oligonucleotide, from mouse to man utilizing novel extraction and quantitation techniques in samples collected from preclinical toxicology studies, a ^{3}H rat ADME study, and a phase 1 clinical trial.

Introduction

Rare genetic disorders have been a challenge to treat by traditional small molecule drugs. The use of antisense oligonucleotides (ASOs) as a platform for drug development to treat these diseases has increased significantly over the years due to their unique mechanism of action at the RNA level (Bennett and Swayze, 2010). ASOs hybridize to their target complementary mRNA, which may alter the site of splicing or result in RNA degradation through RNase H activity, thereby modulating the translation of proteins or eliminating toxic RNA (Crooke, 1999, 2004). Advances in medicinal chemistry have led to several chemical modifications that have been made to improve upon the pharmacokinetic and pharmacodynamic properties of ASOs (Wagner, 1994; Altmann et al., 1996; Lima et al., 1997; Manoharan, 1999). Among the various modifications, the phosphorothioate modification on the phosphodiester backbone structure and the 2′-*O*-(2-methoxyethyl) (2′-MOE) modification on the ribose moiety have consistently demonstrated greater metabolic stability and higher binding affinity to the target mRNA while maintaining RNase H activity by using a chimeric design strategy and decreasing general nonhybridization toxicities ((Manoharan, 1999; McKay *et al.*, 1999; Danis *et al.*, 2001; Yu *et al.*, 2007; Geary, 2009)). These 2′-MOE modifications are commonly known as second generation ASOs. The 2-methoxyethyl modification has led to the development of potent, pharmacologically active, specific ASOs such as mipomersen (marketed as Kynamro), an inhibitor of apolipoprotein B-100 synthesis used to reduce low-density lipoprotein cholesterol, apolipoprotein B, total cholesterol, and non-high-density lipoprotein cholesterol in patients with homozygous familial hypercholesterolemia (Kastelein et al., 2006), and inotersen (marketed as TEGSEDI), an inhibitor of hepatic production of transthyretin protein used to reduce serum transthyretin protein and risk of transthyretin protein deposits in tissues in patients with polyneuropathy caused

N.P., R.Y., S.G., H.G., J.M., and Y.W. are employees and stock holders of Ionis Pharmaceuticals, Inc. E.H. is an employee and stock holder of Akcea Therapeutics.
https://doi.org/10.1124/dmd.119.087395.
This article has supplemental material available at dmd.aspetjournals.org.

ABBREVIATIONS: ADME, absorption, distribution, metabolism, and excretion; APOC3, apolipoprotein C-III; ASO, antisense oligonucleotide; AUC, area under the curve; LC-MS/MS, liquid chromatography–tandem mass spectrometry; 2′-MOE, 2′-*O*-(2-methoxyethyl); MS, mass spectrometry; TBAA, tributylammonium acetate.

by hereditary transthyretin-mediated amyloidosis (Ackermann et al., 2016; Benson et al., 2018; Shen and Corey, 2018).

Volanesorsen, a 20-nucleotide partially 2′-MOE–modified ASO gapmer, was developed to inhibit apolipoprotein C-III (APOC3), a key player in the metabolism of triglycerides and triglyceride-rich lipoproteins. Overexpression of the gene encoding APOC3 is associated with hypertriglyceridemia, while loss-of-function mutations in APOC3 are associated with low triglyceride levels and a decreased risk for cardiovascular disease (Graham et al., 2013; Yang et al., 2016). Patients with an overexpression of APOC3 can have triglyceride levels higher than ~1000 mg/dl and are associated with an increased risk for pancreatitis (Schmitz and Gouni-Berthold, 2018). Treatment with volanesorsen leads to a robust decrease in both APOC3 production and triglyceride concentrations (Pechlaner et al., 2017) and has recently been approved by the European Union as a novel, first-in-class treatment of reduction of triglyceride levels in patients with familial chylomicronemia syndrome. The pharmacokinetic and metabolism properties of volanesorsen have been thoroughly characterized across species from mice to man, including the metabolism in mice and monkeys as part of toxicology studies, in rats using radiolabeled materials, and in humans from a phase 1 healthy volunteer study. The results of these studies are described and compared across species. Additionally, the renal excretion of all ASO metabolite species is reported. This compilation represents a complete metabolism profile for a partially 2′-MOE–modified ASO.

Materials and Methods

Test Compound

Volanesorsen (also called ISIS 304801, ISIS-ApoCIII$_{Rx}$ and IONIS-ApoCIII$_{Rx}$) is a 20-base phosphorothioate oligonucleotide with five 2′-MOE–modified ribofuranosyl nucleotides flanking on both the 5′- and 3′-ends of the unmodified DNA oligonucleotide gap (Fig 1). Full-length purity results of the test compound [as determined by liquid chromatography–tandem mass spectrometry (LC-MS/MS)] were 91.1% with 1.6% of the impurities associated with N-1 (deletion sequence). Dosing was performed based on the quantity of the full-length 20-mer oligonucleotide. Radiolabeled volanesorsen was made (AM Chemicals LLC, CA) with a tritium incorporated into the nonexchangeable 5-carbon position of the ribose sugar of one of the deoxy-thymidine nucleotides in the wing portion of the oligonucleotide (Fig. 1) for radiolabel disposition and mass balance studies in rat. The radio-chemical purity of [^{3}H]-volanesorsen was 97.1 and its specific activity was 1956 μCi/mg.

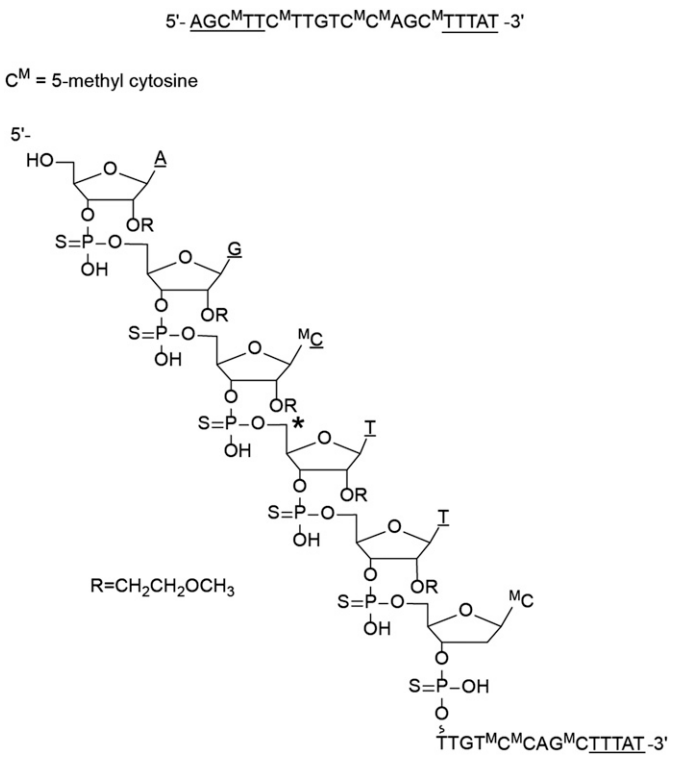

Fig. 1. Sequence and structure of volanesorsen, a phosphorothioate antisense oligonucleotide with 2′-MOE modification at positions 1–5 and 15–20 (underlined). All of the cytosines were 5-methylated and the ^{3}H label was placed on the thymidine (marked with an asterisk) at the ribose C-5 position.

Toxicology Studies in Mice, Rats, and Monkeys

All animal studies were conducted using protocols and methods approved by the Institutional Animal Care and Use Committee and carried out in accordance with the Guide for the Care and Use of Laboratory Animals adopted and promulgated by the United States National Institutes of Health (Bethesda, MD). Male and female CD-1 mice (Charles River Laboratories, Inc., Wilmington, MA) were used in both subchronic (6 or 13 weeks of dosing with 13 weeks of recovery) and chronic studies (26 weeks of dosing with 26 weeks of recovery). Volanesorsen was administered via subcutaneous injections at either 3, 30, or 100 mg/kg dosed every other day for four doses (loading regimen), followed by weekly dosing for 6 weeks; 4, 12, 40, or 100 mg/kg dosed every other day for four doses (loading regimen), followed by weekly dosing for 13 weeks with a 13-week recovery period for the subchronic study; or 3, 10, 30, or 80 mg/kg dosed every third day for three doses (loading regimen), followed by weekly dosing for 26 weeks with a 26-week recovery period for the chronic study. Metabolism was studied at selected samples including 1) peak and trough plasma samples from the subchronic study (1 hour postdose on day 42 and 7 days postdose on day 42, respectively) from animals that received a 30 mg/kg dose; 2) tissues from the subchronic study, including both liver and kidney samples from day 44 to day 93 [i.e., approximately 48 hours after the doses on days 42 and 91, respectively, with a subset of tissues from day 93 also being used for the mass spectrometry (MS) identification study] from animals that received a 12 mg/kg dose and day 182, 13 weeks after the last dose, from animals that were dosed with 100 mg/kg; and 3) urine from the chronic study from 0 to 24 hours and 24–48 hours postdose on day 175 from animals that received the 80 mg/kg dose.

Male and female Sprague-Dawley rats (Charles River Laboratories, Inc.) were used in a 2-year carcinogenicity study. Volanesorsen was administered via subcutaneous injections at 0.2, 1, or 5 mg/kg once weekly for up to 92 days. The plasma pharmacokinetic parameters were studied for all dose levels on the final day of dosing (day 92).

Male and female cynomolgus monkeys (*Macaca fascicularis*; Sierra Biomedical Animal Colony, Sparks, NV) were used in both subchronic and chronic studies as was done in the mice studies. Volanesorsen was administered via subcutaneous injections at either 4, 8, 12, or 40 mg/kg dosed every other day for four doses (loading regimen, with the exception that the first three loading doses for the 4, 8, and 12 mg/kg dosed animals were via 1-hour intravenous infusions), followed by weekly dosing for 13 weeks for the subchronic study; or 3, 6, 12, or 20 mg/kg on days 1, 4, and 7 during week 1 (loading regimen), followed by once weekly dosing for up to 39 weeks for the chronic study. Metabolism was studied in selected samples including: 1) peak and trough plasma samples from the subchronic study [2 hours postdose on day 91 and predose on day 91 (i.e., 7 days postdose on day 84) from animals that received the 8 mg/kg dose]; 2) tissues from the subchronic study including both liver and kidney cortex samples collected on days 44, 93, and 182 (i.e., approximately 48 hours after the dose on day 42, day 91, or 13 weeks after the dose on day 91 from animals that received the 12 mg/kg dose, with a subset of tissues from day 93 also being used for the MS identification study); and 3) urine from the chronic study from 0 to 24 hours and 24–48 hours postdose on day 252 from animals that received the 20 mg/kg dose.

Absorption, Distribution, Metabolism, and Excretion Study in Rats Using [^{3}H]-Volanesorsen

The absorption, distribution, metabolism, and excretion (ADME) of volanesorsen were studied in male and female Sprague-Dawley rats (Charles River Laboratories, Inc.) following a single dose of [^{3}H]-volanesorsen via subcutaneous injection at both 5 and 25 mg/kg, corresponding to 100 and 500 μCi/kg, respectively. The pharmacokinetics, tissue distribution, and mass balance samples were from animals administered a single subcutaneous dose of 5 mg/kg [^{3}H]-volanesorsen, whereas quantitative whole-body autoradiography and additional metabolite profiling and identification samples were from

animals that were administered a single subcutaneous dose of 25 mg/kg [^{3}H]-volanesorsen.

Pharmacokinetics and Metabolism in Humans

A phase 1 clinical study (ISIS 304801-CS1) in healthy male volunteers (age 28–52 years old, weighing between 56.4 and 110.4 kg with a body mass index between 21.1 and 29.6 kg/m^2, $n = 4$ per treatment group, and randomized three active: one placebo, except $n = 4$ active for the 400 mg multiple-dose cohort for day 1) involved either a single subcutaneous injection at 50, 100, 200, or 400 mg, or multiple subcutaneous injections (six total) at 50, 100, 200, or 400 mg on alternating days during the first week (days 1, 3, and 5) and then once a week for the next 3 weeks (days 8, 15, and 22). Metabolism was evaluated in patients who received multiple administrations at 400 mg and included: both peak and trough plasma samples [4 hours postdose on days 22 and 29 (i.e., approximately 7 days postdose on day 22)], and urine samples collected from 0 to 24 hours postdose after the first (day 1) and last (day 22). All subjects provided their written, informed consent. The study protocol was approved by a central institutional review board (Institutional Review Board Services, Canada) and performed in compliance with the standards of good clinical practice and the Declaration of Helsinki in its revised edition.

Analytical Methods

Hybridization Enzyme-Linked Immunosorbent Assay. Plasma concentrations of volanesorsen were determined using a quantitative, sensitive hybridization ELISA method, which is a variation of the method reported previously in Yu et al. (2002). Briefly, hybridization of the complementary sequence of volanesorsen (5′-ATAAAGCTGGACAAGAAGCT-3′, locked nucleic acid modifications are underlined), containing biotin at the 5′-end and digoxigenin at the 3′-end, to the volanesorsen present in plasma, occurs with the hybridized complex subsequently immobilized onto a Neutravidin-coated plate. S1 nuclease is then added to cleave any unhybridized detection probe. The measurement of the hybridized complex attached to the plate is then performed following the addition of antidigoxigenin conjugated to alkaline phosphatase, which catalyzes the conversion of AttoPhos (Promega, Madison, WI) to form the fluorescent product. The reaction was stopped by adding 15% $Na_2HPO_4{\cdot}7H_2O$, and then fluorescence intensity was measured using a fluorescent plate reader. The calibration range of the assay was 1.0–100 ng/ml for the parent compound, with the low end of this range (1.0 ng/ml) defining the lower limit of quantitation. Samples had a maximum dilution of 10,000 to fit into the calibration range. The assay was validated for precision, accuracy, selectivity, sensitivity, and stability of volanesorsen quantitation before analysis of mouse, rat, monkey, and human plasma samples. The assay conducted with synthesized putative shortened oligonucleotide metabolite standards showed no measurable crossreactivity, confirming the assay's specificity for the parent oligonucleotide.

Protein Binding Assay. An ultrafiltration method (Watanabe et al., 2006) was used to determine the extent of plasma protein binding of volanesorsen. Fresh plasma from mouse, monkey, and human was used to evaluate the protein binding at two concentrations (5 and 150 μg/ml) to bracket the C_{max} expected over the dose range evaluated in both preclinical and clinical studies. Aliquots (50 μl per aliquot) of ultrafiltrates (containing unbound volanesorsen) and initial plasma samples [containing total (bound and unbound) volanesorsen] were assayed using the same nuclease-dependent hybridization ELISA method described previously. Then, the percentage of unbound volanesorsen was determined (concentration in ultrafiltrate divided by initial plasma concentration), from which the percentage of bound volanesorsen was calculated. All samples were diluted into pooled human plasma at a minimum of 1:4 for proper running of the ELISA and most samples were diluted greater than 1:4 to fit into the calibration range.

Metabolite Identification Using LC-MS/MS. The selected plasma, tissue, and urine samples from mouse, monkey, and human studies were extracted and analyzed in a similar manner as previously reported (Yu et al., 2016). Briefly, all samples were first homogenized and had the internal standard ISIS 355868 (5′-GCGTTTGCTCTTCTTCTTGCGTTTTTT-3′, a 27-mer phosphorothioate 2′-MOE partially modified oligonucleotide where the 2′-MOE–modified oligonucleotides are underlined) added before extraction. The extraction process was done by first performing a liquid-liquid extraction with phenol/chloroform/isoamyl alcohol (25:24:1), followed by a solid-phase extraction using a 96-well Strata X packed plate (Phenomonex Inc., CA). Samples had an additional pass through a Protein Precipitation Plate (Phenomonex Inc.) before the eluates were dried down under nitrogen at 50°C. Samples were reconstituted with 140 μl water containing 100 μM EDTA.

Samples were analyzed by ion-pairing LC-MS/MS with an Agilent 1100 LC/MS System (Agilent Technologies, Wilmington, DE), in which a loading mobile phase consisting of 25% acetonitrile in 25 mM tributylammonium acetate (TBAA), pH 7.0, was first injected onto a loading column (wide pore C18 guard column, 4 × 2.0 mm; Phenomonex Inc.) before the flow was reversed and the oligonucleotides were separated with an XBridge column (50 mm × 2.1 mm, 2.5 μm particle size, 200 Å pore size; Waters, Milford, MA). The column was equilibrated with 27% acetonitrile in 5 mM TBAA, pH 7.0, and maintained at 55°C with a flow rate of 0.3 ml/min. The samples first passed through a photodiode array detector and UV absorbance was collected at 260 nm before the tandem MS measurement. The single quadrupole mass spectrometer was set to scan a mass-to-charge ratio window of 900–1900 and mass spectra were obtained using a spray voltage of 4 kV, sheath gas flow of 35 psig, drying gas flow rate of 12 l/min at 335°C, and capillary voltage of −150 V. Chromatograms were analyzed using Agilent Chemstation software.

Radiometric Analysis (Liquid Scintillation Counting). Radioactivity in rat samples was quantitated by liquid scintillation counting using a Wallac 1409 automatic liquid scintillation counter (Beckman Coulter, Fullerton, CA). Urine and plasma samples were directly mixed with Ultima Gold LSC Cocktail (PerkinElmer Life and Analytical Sciences, Boston, MA). For solubilized tissue samples, Goldisol (2 ml) was added to each vial. The vials were then incubated overnight (at approximately 50°C for approximately 16 hours). Ultima Gold scintillation cocktail (10 ml) and methanol (1 ml) were added to each vial. Oxygen combustion of feces and bone was carried out using an automatic sample oxidizer. The products of combustion were absorbed in Monophase S for measurement of radioactivity concentrations.

Evaluation of Tritium Exchange. The extent of exchange (%) of the ^{3}H-radiolabel with body water was calculated from the terminal rate constants and area under the curve (AUC) extrapolated to infinity of volatile radioactivity (assumed to be ^3H_2O) using the expression: $100 \times (V{\cdot}k{\cdot}\text{AUC})/D$, where V is the distribution volume of ^3H_2O (in milliliters; exchangeable body water = 60% of body weight) (Richmond et al., 1962), k is the terminal rate constant for ^3H_2O (hour^{-1}; using volatile radioactivity data), AUC is the area under the plasma ^3H_2O (volatile radioactivity) concentration-time curve expressed as nanograms·hour per milliliter, and D is the administered dose (microgram).

Metabolite Profiling by Radio-High-Performance Liquid Chromatography and Identification through Subsequent Fractionation and LC-MS/MS Analysis of [^{3}H]-Volanesorsen Samples. Selected plasma, tissue, and urine samples were extracted using a variation of the method previously reported in Turnpenny et al. (2011). Typically, samples were either mixed with or homogenized in water with 50 μM EDTA. Liquid-liquid extraction was performed by first adding an ammonia solution, followed by phenol/chloroform/isoamyl alcohol (25:24:1). The resulting aqueous extract was further purified by adding dichloromethane, taking the aqueous layer, and then drying it in a centrifugal evaporator and reconstituting it in 200 μl of 50 μM EDTA:5 mM TBAA with 20% acetonitrile (1:1, v/v).

Reconstituted samples were injected on an Agilent 1200 Series HPLC System (Agilent Technologies), which included a LabLogic β-Ram (model 3; LabLogic, Tampa, FL) with a Gilson FC204 fraction collector (Gilson Inc., Middleton, WI) to generate radiochromatograms (or radioactivity profiles). Fractions from the radio-high-performance liquid chromatography were collected in 1-minute intervals and assigned as a region (with 24 regions being collected over the entirety of the run).

Subsequent metabolite identity analysis of the 24 regions was performed using a Waters Acquity HPLC and a Waters Micromass Q-Tof Micro. Samples were injected onto an XBridge Oligonucleotide BEH C18 (2.5 μm, 50 × 2.1 mm, 130 Å column; Waters) with a Phenomenex security guard C18, 4 × 3 mm guard column (Phenomonex Inc.), which was maintained at 60°C with a flow rate of 0.3 ml/min. The column was equilibrated with 400 mM 1,1,1,3,3,3-hexafluoro-2-propanol/15 mM triethylamine and 10% methanol. The MS conditions were set to electrospray ionization in negative mode with a capillary voltage of 2.5 kV, with desolvation gas of nitrogen 500 l/h and cone gas of nitrogen 50 l/h, desolvation temperature at 350°C, a scan range of 400–1500 amu, and a scan rate of 1.0 seconds/scan.

Quantitative Whole-Body Autoradiography. After single subcutaneous doses of [^{3}H]-volanesorsen (25 mg/kg) to four male and four female rats, one male and one female rat were sacrificed at each of the following time points: postdose and 2, 8, 48, and 336 hours. Each carcass was deep frozen in a bath of n-heptane/solid CO_2 at approximately −80°C before being mounted in blocks of carboxymethylcellulose. Radioactive blood standards at concentrations of 3.35, 6.11, 51.9, 554, and 4950 μg equivalents/g were included in

TABLE 1

Quantitation ranges of volanesorsen and selected metabolite calibration curves for plasma and urine (mouse, monkey, and human)

Lower value defined as the lower limit of quantitation and upper value defined as the upper limit of quantitation. Boldface and underlined nucleotides are 2′-O-(2-methoxyethyl)-modified. All of the cytosines were 5-methylated.

Compound Sequence	Description	Backcalculated Calibration Range					
		Mouse Plasma	Monkey Plasma	Human Plasma	Mouse Urine	Monkey Urine	Human Urine
		μg/ml	μg/ml	μg/ml	μg/ml	μg/ml	μg/ml
AGCTTCTTGTCCAGC**TTTAT**	Volanesorsen	0.358–71.6	0.358–71.6	0.358–107.5	0.071–17.9	0.358–71.6	0.035–35.8
AGCTTCTTGTCCAGC**TTTA**	19-mer, 3′-deletion	0.339–67.7	0.339–67.7	0.339–67.7	0.068–16.9	0.336–67.7	0.033–33.9
AGCTTCTTGT	10-mer, 3′-deletion	0.178–35.5	0.176–35.5	0.178–53.3	0.036–8.88	0.176–35.5	0.017–17.8
AGCTT	5-mer, 3′-deletion	0.096–19.3	0.096–19.3	0.482–28.9	0.096–9.63	0.096–19.3	0.009–9.63
CCAGC**TTTAT**	10-mer, 5′-deletion	0.177–35.3	0.177–35.3	0.177–53.0	0.035–8.84	0.177–35.3	0.017–17.7
TTTAT	5-mer, 5′-deletion	0.095–28.5	0.095–28.5	0.190–19.0	0.095–9.51	0.095–28.5	0.009–47.6

each block such that they appeared in each section taken. Sagittal sections (30 μm thickness) were prepared and mounted onto the stage of a macrotome in a cryostat maintained at approximately −20°C. The sections were then exposed to phosphor-imaging plates for 7 days (stored in a lead-lined box), after which the plates were scanned using a FLA5000 radioluminography system. Images were generated using validated TINA radioactivity image data capture software and quantified using validated Seescan2 densitometry software.

Relative Abundance of Volanesorsen and Metabolite Concentration Calculations. The concentrations of volanesorsen and its metabolites in plasma and urine were determined using six calibration curves, one for parent volanesorsen and five for metabolites; the five metabolites chosen were a 19-mer from a 3′-deletion (ISIS 489608), the two 10-mers from both 3′- and 5′-deletions (ISIS 489609 and ISIS 489610, respectively), and the two 5-mer wings from both 3′- and 5′-deletions (ISIS 489611 and ISIS 489612, respectively). A curve for each compound was made in each matrix to use for its respective quantitation (Table 1). If there was not an identical curve for a metabolite, then a curve of the closest metabolite with the same most abundant charge state was used as a surrogate. The concentration of total oligonucleotide in plasma and urine samples was calculated as the sum of concentrations of the parent volanesorsen and its quantitated chain-shortened oligonucleotides; relative abundance (%) was calculated as the concentration of each oligonucleotide divided by the concentration of total oligonucleotide multiplied by 100.

In tissues, the relative abundance of the parent ASO and its metabolites was estimated by dividing the area of individual UV peaks identified as ASOs, through comparison with known standards, by the summed area of all peaks and multiplying by 100. Sample concentrations of each oligonucleotide below the limit of quantification were listed as "0" and treated as "0" in calculating relative abundance. There were no readily apparent gender differences in the abundance of metabolites observed in any samples; therefore, the abundance of these moieties in plasma and urine was summarized by time point with gender combined for mouse, monkey, and human.

Percentage of Dose Excretion Calculations. The percentage of dose excreted of the parent drug and of the sum of all detectable ASO-related species was calculated in mouse, monkey, and human urine. Molar concentrations of volanesorsen and all related metabolites were calculated based on their mass concentration (nanograms per milliliter) divided by their calculated molecular weight. Each volanesorsen molecule produces two wing moieties of variable lengths whose volanesorsen-equivalent concentrations were calculated as their molar concentration divided by 2. Metabolites less than or equal to four bases long were too short to be detected, creating the exception for metabolites from the other wing of those metabolites (i.e., metabolites that were 16–19 bases long), which did not warrant dividing their molar concentration by 2. The amount of volanesorsen and each individual metabolite (micromoles) and volanesorsen-equivalent concentrations of each metabolite (micromole) was calculated using the following equation:

$$Ae_t = C_{urine} \cdot V_{urine} / 1,000,000$$

where, Ae_t is the amount (micromoles) of volanesorsen, each metabolite, or volanesorsen-equivalent excreted up to 24 hours; C_{urine} is the urine concentration (nanomolars) of volanesorsen or individual metabolite of volanesorsen; and V_{urine} is the total urine volume (milliliters) excreted over the 24-hour collection interval.

The amount of total oligonucleotide excreted in rat urine following the 24-hour collection interval was calculated as the sum of the amount (micromoles) of volanesorsen and each metabolite. The percentage of the administered dose excreted in urine was then calculated from the following expression:

$$\%\text{Dose Excreted} = [Ae_{t,\,e.q.}/\text{Administered Dose}] \times 100\%$$

where, $Ae_{t,e.q.} = Ae_t/2$ for metabolites 15 bases long and shorter; $Ae_{t,e.q.}$ is the amount of volanesorsen-equivalent excreted up to 24 hours (micromoles); and Administered Dose (micromoles) is calculated by dose (milligrams) multiplied by 1000 and divided by molecular weight.

Results

Plasma Protein Binding

Volanesorsen is similarly highly bound to plasma proteins in mice, monkeys, and humans. The extent of protein binding is greater than 98% at 5 μg/ml and slightly lower at 150 μg/ml (still greater than 97%) in all three species (Table 2).

Plasma Pharmacokinetic Profiles in Mice, Rats, Monkeys, and Humans

The volanesorsen pharmacokinetic results following single- and multiple-dose subcutaneous administrations in mice, rats, monkeys, and humans all showed multiphasic plasma concentration-time profiles, with a rapid distribution phase and a slower apparent elimination phase. Select pharmacokinetic parameters are shown for the lower dosed, clinically relevant animal studies along with the human parameters in Table 3. Plasma concentrations of volanesorsen generally peaked at 0.5 hours in mice, 1 hour in rats, 1–4 hours in monkeys, and 2–6 hours in humans (Supplemental Fig. 1).

There was little or no accumulation in either man or monkey in mean plasma C_{max} or AUC after repeated doses, and plasma elimination half-lives were similar [monkeys, 12.7–36.2 days; humans, 11.7–31.2 days (over all of the doses measured)], reflecting slow metabolism and elimination from the tissues. The apparent half-lives of [^{3}H]-volanesorsen in rat plasma and blood were approximately 1.26 and 4.96 days, respectively, which are likely underestimates due

TABLE 2

Plasma protein binding in mouse, monkey, and man

Values are an average of three measurements ± S.D.

Nominal Plasma Volanesorsen Concentration	Extent of Plasma Protein Binding		
	Human	Monkey	Mouse
μg/ml	%	%	%
5	99.24 ± 0.07	99.78 ± 0.04	98.12 ± 1.10
150	98.01 ± 0.14	99.48 ± 0.08	97.19 ± 0.47

TABLE 3

Comparison of selected pharmacokinetic parameters across species of volanesorsen following subcutaneous injections

Plasma pharmacokinetic parameters [mean ± S.D.; T_{max}, median (minimum-maximum)] for mice and rats were calculated by noncompartmental methods using the sparse sampling function. Rat (^{3}H)-volanesorsen study concentrations are expressed as microgram equivalents of volanesorsen per milliliter.

Species	Dose Level	Profile Day	Number of Doses	T_{max}	C_{max}	$AUC_{0-24\ h}$	$AUC_{0-48\ h}$	$t_{1/2}$	CL/F[a]
				h	*μg/ml*	*μg·h/ml*	*μg·h/ml*	*day*	*ml/h·kg*
Mouse	3 mg/kg	1	1	0.5	2.18	NC	3.34	NC	897
		42	9	0.5	2.13	NC	4.81	NC	623
Rat	0.2 mg/kg	92	14	1	0.0362	0.234	0.295	NC	469
	1 mg/kg	92	14	0.5	0.771	2.97	3.39	NC	223
	5 mg/kg	92	14	1	12.1	43.1	48	NC	70.2
Rat (^{3}H) Plasma	5 mg/kg	1	1	1	6.96	34.5	40.8	1.26	97.7
Blood	5 mg/kg	1	1	1	5.13	26.2	29.8	4.95	104
Monkey	3 mg/kg	1	1	2 (1 to 2)	9.78 ± 1.86	42.6 ± 6.05	45.4 ± 6.26	12.7[b]	67.3 ± 9.16
		182	28	2 (1 to 2)	6.76 ± 1.53	49.6 ± 8.22	60.4 ± 11.4	NC	51.2 ± 10.6
		273	41	2 (1–4)	4.03 ± 2.23	34.7 ± 14.1	43 ± 17.8	NC	78.6 ± 25.4
	4 mg/kg	42	9	3 (1–4)	12.1 ± 4.20	NC	83.3 ± 15.6	NC	49.5 ± 8.89
		91	16	3 (2–8)	12.5 ± 3.68	NC	92.0 ± 29.8	NC	46.5 ± 11.4
Human	100 mg	1	1	4 (3–6)	2.05 ± 0.979	20.9 ± 5.53	NC	NC	NC
		22	6	3 (3 to 4)	2.9 ± 1.43	24.5 ± 9.32	NC	18.2 ± 10.8	54
	200 mg	1	1	2 (1.5–3)	4.01 ± 0.814	49.1 ± 1.68	NC	NC	NC
		22	6	3 (3 to 4)	4.12 ± 0.72	50.7 ± 6.48	NC	11.7 ± 3.2	41.5
	400 mg	1	1	3.5 (1.5–4)	10.2 ± 3.06	128 ± 40.3	NC	NC	NC
		22	6	4 (3–6)	9.56 ± 3.52	122 ± 39.8	NC	13.9 ± 5.0	31

$AUC_{0-24\ h}$, AUC from 0 to 24 hours; $AUC_{0-48\ h}$, AUC from 0 to 48 hours; CL, clearance; F, bioavailability; NC, not calculated; PK, pharmacokinetic; T_{max}, time to reach C_{max}.

[a] $CL_{0-48\ h}/F$ = [dose (mg/kg)/AUC_{0-48h} (μg*h/ml)] × 1000 for mouse. $CL_{0-168\ h}/F$ = [dose (mg/kg)/$AUC_{0-168\ h}$ (μg*h/ml)] × 1000 for rat. $CL_{0-48\ h}/F$ = [dose (mg/kg)/$AUC_{0-48\ h}$ (μg*h/ml)] × 1000 for monkey. $CL_{0-48\ h}/F$ = [dose (mg/kg)/$AUC_{0-24\ h}$ (μg*h/ml)] × 1000 for human.

[b] Half-life reported in monkeys is for the 8 mg/kg group, which was the lowest dose that could be calculated.

to several concentrations that were below the limit of quantitation in the elimination phase. The tritium label placed in volanesorsen (Fig. 1) was stable; the extent of tritium exchange was only 1.5% of the dose (data not shown). When incorporated into the gap of a 2′-MOE partially modified oligonucleotide, there is extensive exchange with water; however, when incorporated into the wing, the amount of exchange with water is drastically reduced (Ionis internal data).

Metabolite Identification and Quantitation in Mouse, Monkey, and Human

Plasma. Volanesorsen was the most abundant oligonucleotide in both mouse and monkey plasma samples, accounting for >96% in the distribution phase (1 hour postdose) and >63% of the total oligonucleotides in the postdistribution phase (7 days postdose) in mouse, and accounting for >98% of the total oligonucleotides at both the distribution phase (2 hours postdose) and postdistribution phase in monkey. Similar to mouse and monkey plasma, volanesorsen was the major component in human plasma samples and accounted for >99% of total detected oligonucleotides at both the distribution phase (4 hours postdose) and postdistribution phase.

Tissues. In mouse liver and kidney tissue samples taken 48 hours after 13 weeks of treatment (day 93), volanesorsen was the most abundant oligonucleotide and accounted for >70% of the total oligonucleotides. Metabolites consistent with both initial exonuclease-mediated cleavage (N-1 to N-3 metabolites, 17–19 nucleotides in length) and endonuclease-mediated cleavage (N-5 to N-14, 6–15 nucleotides in length) were evident in both liver and kidney samples, with the N-1 (or 19-mer) as the most abundant. Initial profiling using the UV chromatograms indicated that the N-15 (5-mer) metabolites were not present in the samples; however, when samples were run with a more sensitive method (via LC-MS/MS), both 5-mers were able to be detected, although at a low abundance. Metabolites from both exo- and endo-nuclease-mediated metabolism increased from the time treatment ended after 13 weeks (day 93) to the recovery time point (day 182). After 13 weeks of recovery the amount of volanesorsen had decreased to <50% of the total oligonucleotides.

Monkey liver and kidney tissue samples taken 48 hours after 13 weeks of treatment (day 93) exhibited a similar metabolism profile to mice, including volanesorsen being the most abundant oligonucleotide detected (>82% of total oligonucleotides). Metabolites consistent with exonuclease-mediated cleavage were evident in all liver and kidney cortex samples as well as low levels of putative endonuclease metabolism products. After 13 weeks following the last day of treatment the amount of volanesorsen decreased to 48%–52% of total oligonucleotides.

Urine. Mouse, monkey, and human urine samples all had metabolites consistent with both exo- and endo-nuclease-mediated metabolism. The extent of metabolites compared with intact volanesorsen was much greater for all urine samples, with the exception of mouse urine at the 0–24 hour time point. The most abundant individual metabolite in most of the samples were the 7-mers (generated either from 3′- or 5′-deletions). Two metabolites were found in human urine that were not found in mouse or monkey urine, the 18-mer from a 5′-deletion and the 16-mer from a 5′-deletion; however, both were at a very low level (<0.1% of total oligonucleotide excreted over 24 hours). Figure 2 compares selected metabolic profiles in plasma, tissues (mouse and monkey), and urine across the three species.

Excretion. In mice, the mean urinary excretions of intact volanesorsen at 80 mg/kg during 0–24 and 24–48 hours were 60.9% and 4.7%, respectively, whereas total excretions of parent and metabolites over the same period were 74.2% and 16.3%. In monkeys, the mean urinary excretions of intact volanesorsen at 20 mg/kg during 0–24 and 24–48 hours were 2.66% and 1.46%, respectively, whereas the total excretions over the same period were 14% and 5.5%. In humans, the urinary excretion of intact volanesorsen at an average of 5.7 mg/kg (assuming a 70 kg mean body weight) within the first 24 hours following the last dose on day 22 (at near steady state) was very low, 3.23% at the 400-mg dose. Total excretion over the same period was 16.5%. Table 4 compares the percentages of dose excreted across species.

Distribution, Metabolite Identification, Excretion, and Mass Balance in Rat

Plasma. Radiochromatograms from rat plasma samples at C_{max} (2 hours postdose) and 24 hours postdose, at both the 5 and 25 mg/kg dose

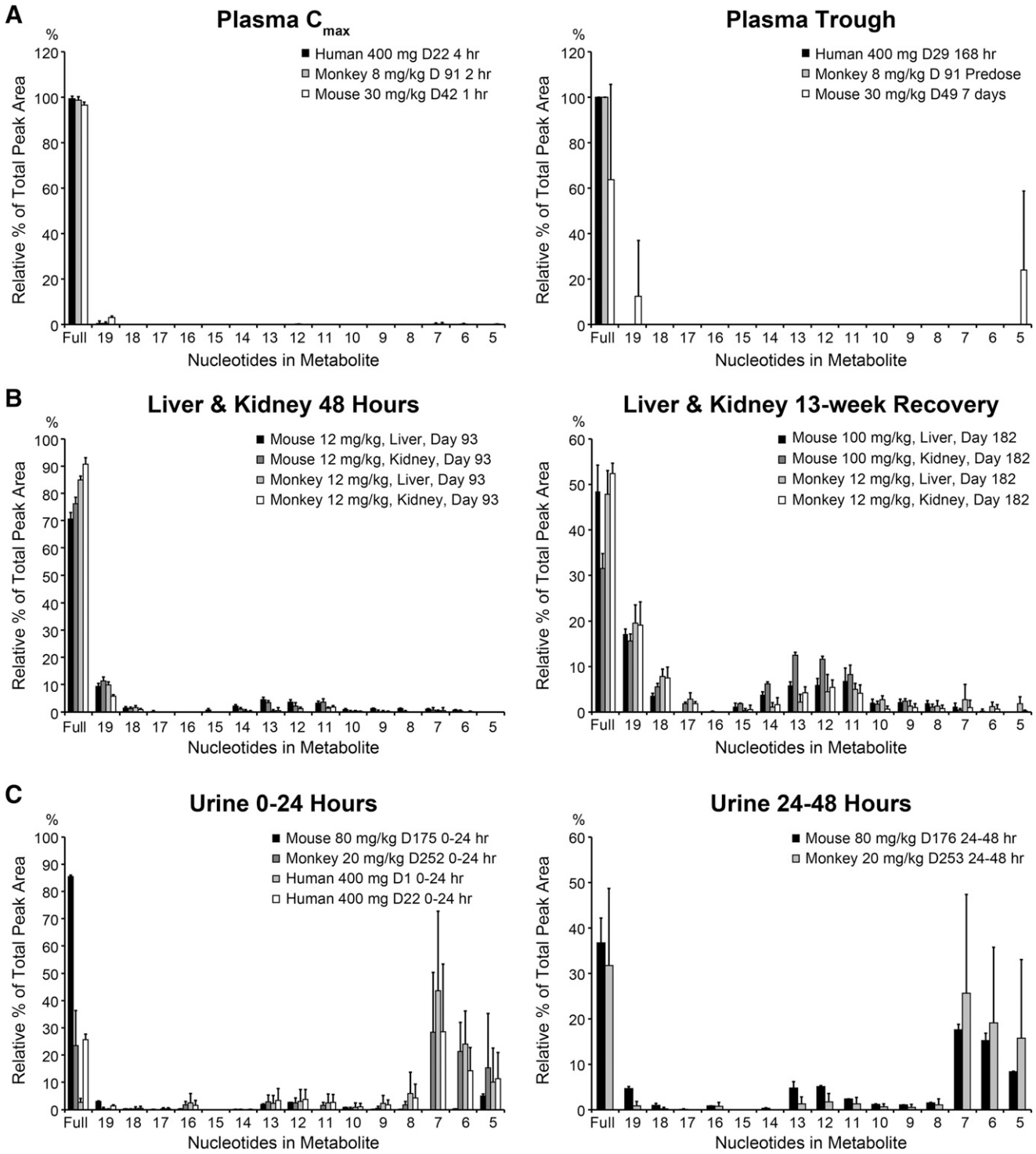

Fig. 2. Comparison of percentage of relative abundance of metabolites in mouse, monkey, and human plasma at C_{max} and trough (A); (B) mouse and monkey liver and kidney 48 hours postdose and 13 weeks after the final dose (B); and mouse, monkey, and human urine from 0 to 24 hours after single or multiple doses and mouse and monkey 24–48 hours after multiple doses (C). Each bar represents the average of two to six measurements. Error bars are the S.E.M.

levels, were qualitatively similar at both dose levels, and at 2 hours postdose the only major circulating radioactive component was volanesorsen, which accounted for 64%–71% of the sample radioactivity. At 24 hours postdose neither intact volanesorsen nor its metabolites were able to be positively identified in the plasma samples.

Tissues. Radioactivity profiles from liver and kidney samples were obtained at 24 hours after administration at both dose levels of 5 and 25 mg/kg. The radioactivity profiles from liver samples at both dose levels were similar, with volanesorsen being the only positively identified ASO, which accounted for 56% and 68%–79% of the sample radioactivity from the low- and high-dose groups, respectively. Sample radiochromatograms contained up to 14 regions (of the 24 total regions) where the radioactivity levels were above the limit of quantification; however, no metabolites

TABLE 4

Percentage of dose excreted (volanesorsen and volanesorsen equivalent) for mice, monkeys, humans, and rats

Species	Dose Level	Dose	Study Day	Time Point	Sum of Oligonucleotide	Dose Excreted Total	Dose Excreted Parent
		μM			μM	%	%
Mouse	80 mg/kg	0.279	176	24 h	0.129[a]	46.4[a]	37.6[a]
					0.285[a]	101.9[a]	84.2[a]
				Mean	0.207	74.2	60.9
Mouse	80 mg/kg	0.279	177	48 h	0.031	10.9	3.65
					0.061	21.7	5.75
				Mean	0.046	16.3	4.7
Monkey	20 mg/kg	6.979	253	24 h	1.438	20.6	1.60
					0.405	5.81	0.99
					1.095	15.7	5.39
				Mean (S.D.)	0.980 (0.526)	14.0 (7.5)	2.7 (2.4)
Monkey	20 mg/kg	6.979	254	48 h	0.539	7.72	0.89
					0.077	1.10	0.41
					0.542	7.76	3.08
				Mean (S.D.)	0.386 (0.267)	5.5 (3.8)	1.5 (1.4)
Human	400 mg	55.832	1	24 h	17.016	30.5	0.52
					8.542	15.3	0.23
					12.009	21.5	0.13
					4.737	8.48	0.29
				Mean (S.D.)	10.58 (3.64)	18.9 (6.5)	0.3 (0.1)
Human	400 mg	55.832	22	24 h	2.356	4.22	0.78
					15.553	27.9	4.96
					9.752	17.5	3.95
				Mean (S.D.)	9.22 (6.61)	16.5 (11.8)	3.2 (2.2)
Rat	5 mg/kg	0.349	1	24 h	0.043	12.5	0.33[a]
					0.045	12.9	NA
					0.044	12.5	NA
				Mean (S.D.)	0.044 (0.001)	12.6 (0.2)	NA
Rat	25 mg/kg	1.745	1	24 h	0.399	22.9	2.09
					0.341	19.6	1.34
				Mean	0.370	21.2	1.7

[a]Samples were a pool of three individuals.

were able to be positively identified in the subsequent LC-MS/MS analysis.

The radioactivity profiles from kidney samples were also similar between both dose levels. Sample radiochromatograms contained up to nine regions where the radioactivity was higher than the limit of quantification. Volanesorsen was again the predominant component and accounted for 63% and 59%–62% of the sample radioactivity from the low- and high-dose groups, respectively. Three metabolites were positively identified by MS in kidney samples, yet only two of them had the radiolabel attached; therefore, only those two were used in subsequent calculations. The two with the radiolabel still attached were the 7-mer from a 3′-deletion and the 8-mer from a 3′-deletion. The metabolite detected without the radiolabel was the 6-mer from a 5′-deletion. While the remaining metabolites were also unidentified by mass spectrometry in kidney, the metabolites did make up a larger percentage of total ASO at both dose levels.

Urine. Characterization of rat urine samples from 0 to 6 and 6 to 24 hours postdose from both the 5 mg/kg (pooled) and 25 mg/kg animals showed qualitatively similar radioactivity profiles (for both time intervals and dose levels). The major urinary metabolites (>10% extract radioactivity) were the 6-mer (from a 3′-deletion; 26%–40%) and the 7-mer (from a 3′-deletion; 16%–29%) in all samples analyzed. Intact volanesorsen was also present and accounted for 2.5% and 10.7% from 0 to 24 hours at the 5 and 25 mg/kg doses, respectively. The radiochromatograms had several other regions that were poorly resolved broad areas of radioactivity rather than distinct peaks, and generally each accounted for <5% of the sample radioactivity (Supplemental Fig. 2).

Excretion. In animals administered the 5 mg/kg dose a mean total of 58% of the dose was recovered in the excreta over the 1344 hours postdose, of which the largest proportion (mean of 48%) was recovered in the urine, with 8% recovered in the feces and a further 2% of the dose recovered in cage washings. Excretion of radioactivity was nearly complete by 1344 hours, since a mean of only 0.13% dose remained in the contents of the gastrointestinal tract at this time. Urinary excretion was most rapid during 0–6 hours when 9% of the administered dose was recovered. A further 4% of the dose was recovered during 6–24 hours postdose. Thereafter, 1% of the administered dose was recovered in the urine each day until daily collections ceased at 168 hours. Weekly 24-hour collections from 168 to 1344 hours were extrapolated such that an estimated 4% to 5% of the dose was excreted via the urine each week, up to 6 weeks. The weekly excretion via urine declined to 3% of the dose at 7 weeks and 2% of the dose at 8 weeks. Intact volanesorsen was present at a low level in the urine and accounted for 0.33% of the dose from 0 to 24 hours.

The recovery of radioactivity from excreta over the 0–24 hour collection period from animals administered the higher (25 mg/kg) dose was 20.04%–23.82% of the dose, of which almost all was in the urine (only 0.48%–0.97% of the dose was in the feces). Intact volanesorsen was also present in the urine and was 1.34%–2.09% of the dose (Table 4).

Quantitative Whole-Body Autoradiography. Tissue concentrations of radioactivity at 2, 8, 48, and 336 hours postdose from male and female rats obtained by quantitative whole-body autoradiography were determined and are presented in Fig. 3. Plasma concentrations were lower than the corresponding blood values at 2 and 8 hours postdose but remained measurable at 48 and 336 hours. Consistent with the subcutaneous route of administration, high levels of radioactivity were observed at the dose injection site. With the exception of the dose site, the kidney contained the highest concentrations of radioactivity, followed by the liver, which reached its maximum concentrations at 48 hours postdose. As expected, the brain and spinal cord had little to no radioactivity

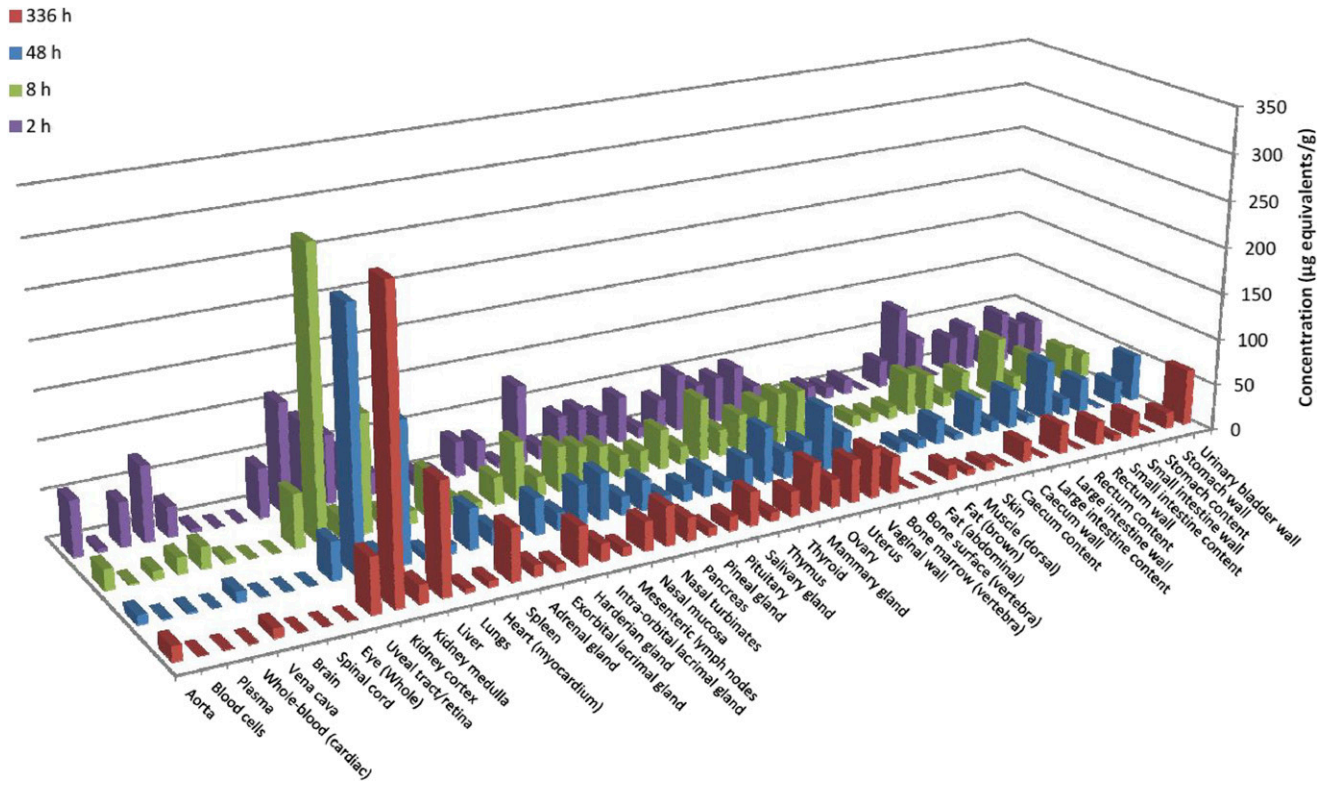

Fig. 3. Concentrations of radioactivity in tissues by quantitative whole-body autoradiography following a single subcutaneous administration of [^{3}H]-volanesorsen at 25 mg/kg to male rats (one animal per time point).

at all time points, due to the inability of the ASO to cross the blood-brain barrier.

Discussion

The pharmacokinetics and metabolism of volanesorsen have been thoroughly investigated across species. In all species, volanesorsen demonstrated dose-dependent and multiphasic plasma concentration-time profiles, with a rapid distribution phase and slower elimination phase. There was little or no accumulation in plasma C_{max} or AUC after repeated doses, and plasma elimination half-lives were similar (2–4 weeks in both monkeys and humans), reflecting slow metabolism and elimination from the tissues. The shorter half-life in rats (1–5 days) was an underestimate due to several concentrations falling below the limit of quantitation in the elimination phase following single-dose administration.

Volanesorsen, like other 2′-MOE partially modified ASOs, has similar tissue distribution characteristics between mice, rats, and monkeys, with the highest concentrations in the liver and kidneys ((Geary et al., 2003; Levin et al., 2007; Yu et al., 2015)). It is generally believed that ASOs distribute into tissues via receptor-mediated endocytosis (Crooke et al., 2017) rather than passive diffusion. Endocytic cellular uptake may be considered to be predominately unidirectional, and in fact very large tissue-to-plasma concentration gradients in ASO concentration (~5000:1) are typically observed in both preclinical species and man (Geary, 2009; Geary et al., 2015; Wang et al., 2018). Slow distribution of ASO back to plasma may correlate with cell turnover (cell death) or a very slow rate of reversible distribution back into plasma from tissue. Further studies are warranted to better understand the effect of ASO chemistry, cell types and turnover, and plasma and tissue protein binding on tissue uptake of ASOs.

2′-MOE partially modified ASOs are slowly metabolized by nucleases in tissues, via predominantly endonuclease hydrolysis at various positions within the deoxyphosphorothioate gap, followed by subsequent 3′- and 5′-exonuclease hydrolysis of the exposed deoxynucleoside ends of the formed metabolites (Fig 4). In plasma, the unbound (and low-binding) chain-shortened oligonucleotide metabolites and any remaining residual unbound (high-binding) parent drug are cleared by glomerular filtration in the kidney, where the parent ASO is mostly reuptaken by renal proximal tubules when the dose is low (uptake is within linear range), serving as a site of metabolism in kidney (Geary *et al.*, 2003; Yu *et al.*, 2007).

Volanesorsen distributes extensively to both liver and kidney tissues. At the dose of 4 mg/kg in monkeys (similar to a 300 mg clinical dose), volanesorsen exposure in kidney cortex was approximately 50% higher than that in the liver. Nonetheless, a parallel elimination phase after the last dose of volanesorsen was observed between kidney cortex and liver. Similar relative proportions of ASO metabolites were observed between the two tissues, suggesting equivalent roles of liver and kidney in ASO metabolism.

Metabolism of volanesorsen was studied in both a ^{3}H-radiolabeled rat ADME study and nonlabeled studies in mice and monkeys. The lack of structural information obtained from the rat ADME study is likely due to having only a single administration of volanesorsen (instead of multiple administrations) and insufficient sample cleanup. The initial extraction method in this study had minimal processing to increase metabolite absolute recovery. The increase in matrix was expected and was planned to be cleaned online, i.e., via the fractionations on the radio-high-performance liquid chromatography. However, much of the matrix coeluted with many of the metabolites (particularly the shorter ones) and was unable to be further processed, leading to signal suppression due to matrix effects. Therefore, even though utilizing a radiolabeled ASO

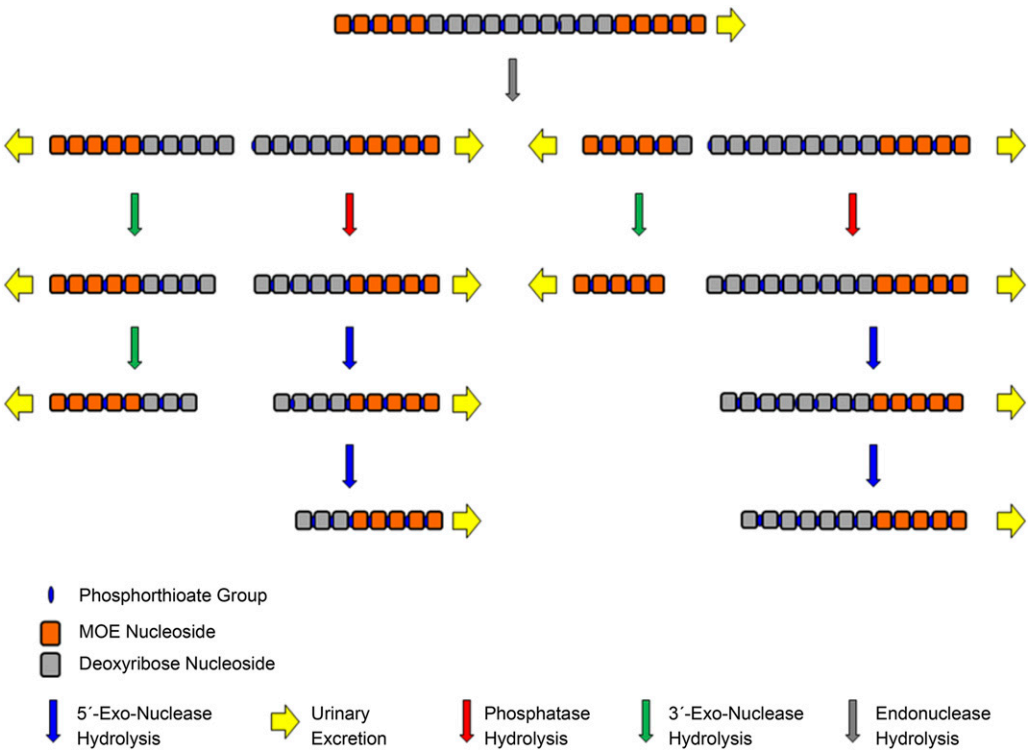

Fig. 4. Metabolic biotransformation and excretion pathways of second generation ASOs.

for the ADME study has many benefits it is apparent that using a single-dose study to examine metabolism for a compound that is extensively distributed to tissues where the metabolism takes place may not be ideal. The study design should be more reflective of the manner in which the drug will be administered in the clinic. However, the overall tissue profiling evaluations demonstrated similarity between the three species, and similar observations would be anticipated in human tissue extracts.

The relative abundance of the parent drug in urine across the evaluated species appears to be related to the dose administered, 80 mg/kg in mice, 20 mg/kg in monkeys, and 400 mg (5.7 mg/kg) in man, with the higher milligram/kilogram dose resulting in greater relative abundance of the parent drug in urine likely attributed to a higher free fraction in plasma or less fraction of volanesorsen being reabsorbed in the proximal tubules at higher dose levels. The total proportion of drug-related moieties eliminated in urine over a 24-hour postdose period in mice, monkeys, and humans at steady state appears generally consistent with urinary elimination being the major excretion pathway for partially 2′-MOE–modified ASOs and their associated metabolites.

It is worth noting that the metabolic profile of volanesorsen in urine differs somewhat from what has been reported for other partially 2′-MOE–modified ASOs. In previous nonradiolabeled urine metabolism studies, ASOs six bases long or less were not detected, as well as ASOs from 15 to 19 bases long, whereas all of those metabolites were found in this study. While the abundance of the longer ASO metabolites are very low, the concentrations of the 5- and 6-mers are quite high. This difference is most likely not due to a difference in metabolism between the previous ASOs and volanesorsen, but instead due to improved extraction methods (Ionis internal data). The previous reports used two-step, solid-phase extraction (a strong anion exchange followed by a C18), which results in very low, absolute recovery of short metabolites (five to seven bases long). The method used in this report has a higher absolute recovery for ASOs ranging from 5 to 20 bases in length and is able to capture the entire metabolic profile much better than before (Geary *et al.*, 2003; Yu *et al.*, 2007). It is likely that the previously reported total ASO recovery in urine for ASOs utilizing these older extraction methods led to an underestimate of the actual value. With these improved methods we were able to generate mass balance data showing approximately 16.5% recovery of the dose administered over a 24-hour postdose interval, which would lead to complete recovery of the administered dose assuming the same excretion on each of the other 6 days of a weekly dose interval (a reasonable assumption considering the long half-life of the ASO in tissues).

Despite improved extraction methods, there are still limitations with LC-MS/MS in achieving the required sensitivity for the detection and quantification of parent ASOs and metabolites at therapeutically relevant doses. Quantitation of ASOs and their metabolites was recently reviewed (Kaczmarkiewicz et al., 2019), and while there have been many advancements in this application, it is still a complex multivariable issue that can make achieving the desired lower limit of quantitation difficult (especially for low trough plasma concentrations, which are often $<$1 ng/ml for metabolites). Interestingly, most published methods employ the use of multiple reactions monitoring for their MS detection and an ion pair that yields a large charge-state distribution. The tactic employed here was to use the ion-pair TBAA to create a narrow charge-state distribution and operate the MS in scan mode, resulting in an increase in the metabolite signals at the expense of the full-length one. This compromise allowed us to characterize every metabolite from 5 to 19 bases in a single run.

Taken together, the ADME characteristics of volanesorsen are similar across the investigated species and are consistent with previous reports of other ASOs of the same chemical class (Geary *et al.*, 2003, 2015, Yu *et al.*, 2007, 2013). Ultimately, these findings were consistent with the main mode of volanesorsen metabolism being initial endonuclease-mediated hydrolysis at various positions within the central gap of the parent compound, followed by subsequent exonuclease (3′ and 5′)-mediated hydrolysis of the deoxynucleoside ends of the formed

metabolites. Moreover, this study also provided results consistent with the primary route of elimination of all volanesorsen-related moieties being urinary excretion.

Acknowledgments

The authors thank Shannon Hall and Christine Hoffmaster for assistance with tracking down essential information needed to complete the manuscript, Scott Henry for support and critical review, and Wanda Sullivan for administrative assistance.

Authorship Contributions

Participated in research design: Post, Yu, Wang.

Conducted experiments: Post.

Performed data analysis: Post, Yu.

Wrote or contributed to the writing of the manuscript: Post, Yu, Greenlee, Gaus, Hurh, Matson, Wang.

References

Ackermann EJ, Guo S, Benson MD, Booten S, Freier S, Hughes SG, Kim TW, Jesse Kwoh T, Matson J, Norris D, et al. (2016) Suppressing transthyretin production in mice, monkeys and humans using 2nd-generation antisense oligonucleotides. *Amyloid* **23**:148–157.

Altmann K-H, Dean NM, Fabbro D, Freier SM, Geiger T, Haner R, Husken D, Martin P, Monia BP, Muller M, et al. (1996) Second generation of antisense oligonucleotides: from nuclease resistance to biological efficacy in animals. *Chimia (Aarau)* **50**:168–176.

Bennett CF and Swayze EE (2010) RNA targeting therapeutics: molecular mechanisms of antisense oligonucleotides as a therapeutic platform. *Annu Rev Pharmacol Toxicol* **50**:259–293.

Benson MD, Waddington-Cruz M, Berk JL, Polydefkis M, Dyck PJ, Wang AK, Planté-Bordeneuve V, Barroso FA, Merlini G, Obici L, et al. (2018) Inotersen treatment for patients with hereditary transthyretin amyloidosis. *N Engl J Med* **379**:22–31.

Crooke ST (1999) Molecular mechanism of antisense drugs: human RNase H. *Antisense Nucleic Acid Drug Dev* **9**:377–379.

Crooke ST (2004) Antisense strategies. *Curr Mol Med* **4**:465–487.

Crooke ST, Wang S, Vickers TA, Shen W, and Liang XH (2017) Cellular uptake and trafficking of antisense oligonucleotides. *Nat Biotechnol* **35**:230–237.

Danis RP, Henry SP, and Ciulla TA (2001) Potential therapeutic application of antisense oligonucleotides in the treatment of ocular diseases. *Expert Opin Pharmacother* **2**:277–291.

Geary RS (2009) Antisense oligonucleotide pharmacokinetics and metabolism. *Expert Opin Drug Metab Toxicol* **5**:381–391.

Geary RS, Norris D, Yu R, and Bennett CF (2015) Pharmacokinetics, biodistribution and cell uptake of antisense oligonucleotides. *Adv Drug Deliv Rev* **87**:46–51.

Geary RS, Yu RZ, Watanabe T, Henry SP, Hardee GE, Chappell A, Matson J, Sasmor H, Cummins L, and Levin AA (2003) Pharmacokinetics of a tumor necrosis factor-α phosphorothioate 2′-*O*-(2-methoxyethyl) modified antisense oligonucleotide: comparison across species. *Drug Metab Dispos* **31**:1419–1428.

Graham MJ, Lee RG, Bell TA III, Fu W, Mullick AE, Alexander VJ, Singleton W, Viney N, Geary R, Su J, et al. (2013) Antisense oligonucleotide inhibition of apolipoprotein C-III reduces plasma triglycerides in rodents, nonhuman primates, and humans. *Circ Res* **112**:1479–1490.

Kaczmarkiewicz A, Nuckowski Ł, Studzińska S, and Buszewski B (2019) Analysis of antisense oligonucleotides and their metabolites with the use of ion pair reversed-phase liquid chromatography coupled with mass spectrometry. *Crit Rev Anal Chem* **49**:256–270.

Kastelein JJ, Wedel MK, Baker BF, Su J, Bradley JD, Yu RZ, Chuang E, Graham MJ, and Crooke RM (2006) Potent reduction of apolipoprotein B and low-density lipoprotein cholesterol by short-term administration of an antisense inhibitor of apolipoprotein B. *Circulation* **114**: 1729–1735.

Levin AA, Yu RZ, and Geary RS (2007) Basic principles of the pharmacokinetics of antisense oligonucleotide drugs, in *Antisense Drug Technology, Principles, Strategies and Applications* (Crooke ST ed) pp 183–215, Taylor & Francis Group, Boca Raton, FL.

Lima WF, Mohan V, and Crooke ST (1997) The influence of antisense oligonucleotide-induced RNA structure on *Escherichia coli* RNase H1 activity. *J Biol Chem* **272**:18191–18199.

Manoharan M (1999) 2′-carbohydrate modifications in antisense oligonucleotide therapy: importance of conformation, configuration and conjugation. *Biochim Biophys Acta* **1489**:117–130.

McKay RA, Miraglia LJ, Cummins LL, Owens SR, Sasmor H, and Dean NM (1999) Characterization of a potent and specific class of antisense oligonucleotide inhibitor of human protein kinase C-α expression. *J Biol Chem* **274**:1715–1722.

Pechlaner R, Tsimikas S, Yin X, Willeit P, Baig F, Santer P, Oberhollenzer F, Egger G, Witztum JL, Alexander VJ, et al. (2017) Very-low-density lipoprotein-associated apolipoproteins predict cardiovascular events and are lowered by inhibition of APOC-III. *J Am Coll Cardiol* **69**: 789–800.

Richmond CR, Langham WH, and Trujillo TT (1962) Comparative metabolism of tritiated water by mammals. *J Cell Comp Physiol* **59**:45–53.

Schmitz J and Gouni-Berthold I (2018) APOC-III antisense oligonucleotides: a new option for the treatment of hypertriglyceridemia. *Curr Med Chem* **25**:1567–1576.

Shen X and Corey DR (2018) Chemistry, mechanism and clinical status of antisense oligonucleotides and duplex RNAs. *Nucleic Acids Res* **46**:1584–1600.

Turnpenny P, Rawal J, Schardt T, Lamoratta S, Mueller H, Weber M, and Brady K (2011) Quantitation of locked nucleic acid antisense oligonucleotides in mouse tissue using a liquid-liquid extraction LC-MS/MS analytical approach. *Bioanalysis* **3**:1911–1921.

Wagner RW (1994) Gene inhibition using antisense oligodeoxynucleotides. *Nature* **372**:333–335.

Wang S, Allen N, Vickers TA, Revenko AS, Sun H, Liang XH, and Crooke ST (2018) Cellular uptake mediated by epidermal growth factor receptor facilitates the intracellular activity of phosphorothioate-modified antisense oligonucleotides. *Nucleic Acids Res* **46**: 3579–3594.

Watanabe TA, Geary RS, and Levin AA (2006) Plasma protein binding of an antisense oligonucleotide targeting human ICAM-1 (ISIS 2302). *Oligonucleotides* **16**:169–180.

Yang X, Lee SR, Choi YS, Alexander VJ, Digenio A, Yang Q, Miller YI, Witztum JL, and Tsimikas S (2016) Reduction in lipoprotein-associated apoC-III levels following volanesorsen therapy: phase 2 randomized trial results. *J Lipid Res* **57**:706–713.

Yu RZ, Baker B, Chappell A, Geary RS, Cheung E, and Levin AA (2002) Development of an ultrasensitive noncompetitive hybridization-ligation enzyme-linked immunosorbent assay for the determination of phosphorothioate oligodeoxynucleotide in plasma. *Anal Biochem* **304**:19–25.

Yu RZ, Graham MJ, Post N, Riney S, Zanardi T, Hall S, Burkey J, Shemesh CS, Prakash TP, Seth PP, et al. (2016) Disposition and pharmacology of a GalNAc3-conjugated ASO targeting human lipoprotein (a) in mice. *Mol Ther Nucleic Acids* **5**:e317.

Yu RZ, Grundy JS, and Geary RS (2013) Clinical pharmacokinetics of second generation antisense oligonucleotides. *Expert Opin Drug Metab Toxicol* **9**:169–182.

Yu RZ, Grundy JS, Henry SP, Kim TW, Norris DA, Burkey J, Wang Y, Vick A, and Geary RS (2015) Predictive dose-based estimation of systemic exposure multiples in mouse and monkey relative to human for antisense oligonucleotides with 2′-*O*-(2-methoxyethyl) modifications. *Mol Ther Nucleic Acids* **4**:e218.

Yu RZ, Kim TW, Hong A, Watanabe TA, Gaus HJ, and Geary RS (2007) Cross-species pharmacokinetic comparison from mouse to man of a second-generation antisense oligonucleotide, ISIS 301012, targeting human apolipoprotein B-100. *Drug Metab Dispos* **35**:460–468.

Address correspondence to: Noah Post, Ionis Pharmaceuticals, Inc., 2855 Gazelle Court, Carlsbad, CA 92010. E-mail: npost@ionisph.com